PHONONIC AND ELASTIC PROPERTIES OF $TlInTe_2$ AND $TlGaTe_2$ CRYSTALS: EXPERIMENT AND FIRST-PRINCIPLES CALCULATIONS

Z.A. JAHANGIRLI[1,2], I.A. MAMEDOVA[1], A.I. NAJAFOV[1], G.R. MAHMUDOVA[1], V.B. ALIYEVA[1], Z.I. BADALOVA[1], T.G. MAMMADOV[1], and N.A. ABDULLAYEV[1,2]*

[1]Institute of Physics of the Ministry of Science and Education of Azerbaijan, Baku, Azerbaijan
[2]Baku State University, Baku, Azerbaijan
**e-mail: abnadir@mail.ru*

The phonon properties of $TlInTe_2$ and $TlGaTe_2$ crystals were studied experimentally by Raman scattering and theoretically from first principles using density functional theory (DFT). Raman scattering studies were used to determine the frequencies of Raman-active optical modes. Phonon mode dispersion, the origin of energy states, the projected partial densities of states (PDOS) onto atoms, and optical phonon frequencies were calculated from first principles. Six elastic constants (C_{11}, C_{12}, C_{13}, C_{33}, C_{44}, and C_{66}) of the $TlInTe_2$ and $TlGaTe_2$ crystal compounds were also calculated, and the bulk modulus, shear moduli, Young's moduli, and Poisson's ratio were determined.

Keywords: Raman scattering, optical phonons, first principles, phonon dispersion, elastic constants, elastic modules, Poisson's ratio.
DOI:10.70784/azip.1.2025403

1. INTRODUCTION

Semiconductor compounds $TlInTe_2$ and $TlGaTe_2$ belong to the group of compounds with the structure of the TlSe type and are characterized by a centrosymmetric tetragonal structure with the space group of symmetry (*I4/mcm*) [1, 2]. In these compounds, trivalent ions of a metal M (In3+ or Ga3+) are tetragonally surrounded by Te^{2-} ions, and monovalent Tl^{+} ions are surrounded by eight Te^{2-} ions (Fig. 1). Thus, long negatively charged chains are formed that are stretched along the crystallographic axis. Fragments of various chains are bound by monovalent Tl+ ions located between them. There is covalent bonding inside the chains, and the chains themselves are bound with each other by weaker ionic bonds. It is this anisotropy that leads to assigning compounds with the TlSe type structure to one-dimensional (1D) materials. The structure of the compounds like $TlGaTe_2$ is stable against high hydrostatic pressure [3–5]. For example, $TlInTe_2$ does not suffer structural PTs at the pressure of at least up to 33.5 GPa while undergoing a semiconductor–semimetal transition at 4 GPa with a subsequent transition to the superconducting state at 5.7 GPa (Tc = 3.8 K) [3].

Recently, the $TlInTe_2$ and $TlGaTe_2$ compounds and their structural analogues have been extensively studied, since, in addition to their promising applications in optoelectronics and photovoltaics [6, 7], they were found to exhibit, at room temperature, local deformation of the crystal surface relief under laser were found to exhibit, at room temperature, local deformation of the crystal surface relief under laser irradiation [8], low lattice heat conductivity (~0.5 W/mK) [9–12], and specific electroconductivity features [13]. In structural analogues of these compounds—$TlInSe_2$ crystals—a high Seebeck coefficient (107 mkV/K) is observed, which correlates with the formation of an incommensurate superlattice in them [14].

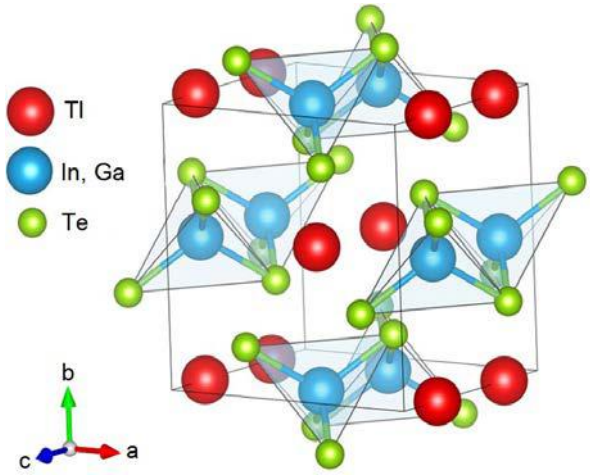

Fig. 1. Schematic diagram of the tetragonal crystal structure of $TlMTe_2$ compounds (M=In, Ga).

131, H.Javid ave, AZ-1073, Baku
Institute of Physics
E-mail: jophphysics@gmail.com

In this article, we present the results of an experimental and theoretical study from first principles of Raman spectra and elastic properties of $TlGaTe_2$ and $TlInTe_2$ crystals.

2. EXPERIMENTAL AND CALCULATION METHODS

$TlGaTe_2$ and $TlInTe_2$ compounds were synthesized by direct single-temperature synthesis from elements with a purity of at least 99.999% in Stepanov quartz vessels evacuated to 10^{-2} Pa. Single crystals of the studied compounds were obtained by directional crystallization.

The resulting crystals were characterized by X-ray diffraction and Raman scattering.

X-ray diffraction studies of the obtained samples were performed on a "D2 Phaser" X-ray diffractometer using CuK_α radiation at T = 300 K. Phase analyses were performed by the Rietveld method using standard EVA and TOPAS-4.2 programs (Bruker, Germany). The lattice parameters of the studied crystals were determined with an accuracy of ±0.001 Å. The details of the X-ray diffraction studies have been described in detail in our previous works [15-17].

The Raman scattering study in $TlGaTe_2$ and $TlInTe_2$ crystals was carried out at a temperature of T = 300 K on samples with a mirror surface, in backscattering geometry, using a "Nanofinder 30" confocal Raman microspectrometer (Tokyo Instr., Japan). YAG:Nd laser with a second harmonic wavelength of λ = 532 nm was used as the excitation light source. The diffraction grating of 1800 lines/mm was used in the spectrometer measurements, with which the accuracy of determining the spectral line positions was no worse than 0.5 cm^{-1}. The experimental technique used to study the Raman spectra is described in detail in [18–23]. Ab-initio calculations of the lattice dynamics were performed using density functional perturbation theory (DFPT) [24–26] using the plane-wave pseudopotential method implemented in the ABINIT code [27]. In this work, norm-preserving Hartwigsen-Goedecker-Hutter pseudopotentials were used [28]. The exchange-correlation interaction was described in the generalized gradient approximation (GGA) [29].

Plane waves with energies up to 80 Ry were taken into account in the expansion of the wave functions, ensuring good convergence of the total energy. Summations over the ZB were performed on a 4×4×4 Monkhorst-Pack grid [30]. The lattice parameters and equilibrium positions of atoms in the unit cell were determined by minimizing the Hellman-Feynman forces. Equilibrium positions of atoms in the unit cell were found using the Broyden–Fletcher–Goldfarb–Shanno (BFGS) method, using experimental data as initial values. The minimization process was continued until the force moduli were less than 10^{-8} Ry/Bohr. A 40x40x40 grid of points in the BZ was used to calculate the phonon density of states. To obtain the LO-TO splitting at the center of the BZ for polar modes, the long-range Coulomb field was taken into account, and a nonanalytical term, which depends on the Born effective charge tensors and the electron permittivity, was added to the dynamic matrix. The dependence of the convergence of the total energy and Hellman-Feynman forces on the Monkhorst-Pack grid and on the maximum energy of plane waves, taking into account the optimal computer time used for calculations, showed that the 4×4×4 grid and the maximum energy of plane waves of 80 Ry in the expansion of wave functions give fairly good results.

3. RESULTS AND DISCUSSION

3.1. Optical Phonons in $TlGaTe_2$ and $TlInTe_2$ Crystals

The unit cell of $TlGaTe_2$ and $TlInTe_2$ contains two formula units, i.e., there are 8 atoms. Accordingly, the vibrational spectrum consists of 24 lattice modes and is described by the following irreducible representations at the center of the Brillouin zone [31]:

$$\Gamma = A^1_g + 2A_{2g} + 3A_{2u} + B_{1g} + B_{1u} + 2B_{2g} + 3E_g + 4E_u \quad (1)$$

Of these, three modes are acoustic, the A_{2u} and E_u modes are IR-active, the E_g, B_{2g}, A_{1g}, and B_{1g} modes are Raman (R)-active, and the B_{1u} and A_{2g} modes are so-called silent modes. The E modes are doubly degenerate.

The Raman spectra of $TlGaTe_2$ and $TlInTe_2$ are shown in Figure 2. The frequencies of the Raman-active modes that we recorded are in good agreement with the experimental results [31, 32, 33]. Table 1 lists the frequencies of the Raman-active modes in $TlGaTe_2$ and $TlInTe_2$ crystals recorded in this work. For comparison, the table also lists the frequencies of these modes determined experimentally in [31, 32, 33], as well as those calculated theoretically in [6, 9, 32] and in this work (Section 1).

As can be seen from Fig. 3a, the dispersion of optical phonons in all symmetric directions, except for the PN line, is insignificant, indicating weak interatomic interaction in these directions. In addition, the presence of lighter Ga atoms shifts the phonon spectra of the $TlGaTe_2$ compound towards higher frequencies (>200 cm^{-1}). From the partial phonon densities of states of the $TlInTe_2$ and $TlGaTe_2$ crystals shown in Fig. 3b, it is evident that the main contribution at low frequencies is made by the heaviest atoms (marked Tl in red), at medium frequencies by Te atoms (blue), and at high frequencies by In and Ga atoms (green). Analysis of the calculation results (Fig. 3b) indicates that the substitution of gallium atoms for indium atoms in $TlGa_xIn_{1-x}Te_2$ should experimentally manifest itself in behavior with a change in the composition of the ^2E_g and ^3E_g modes.

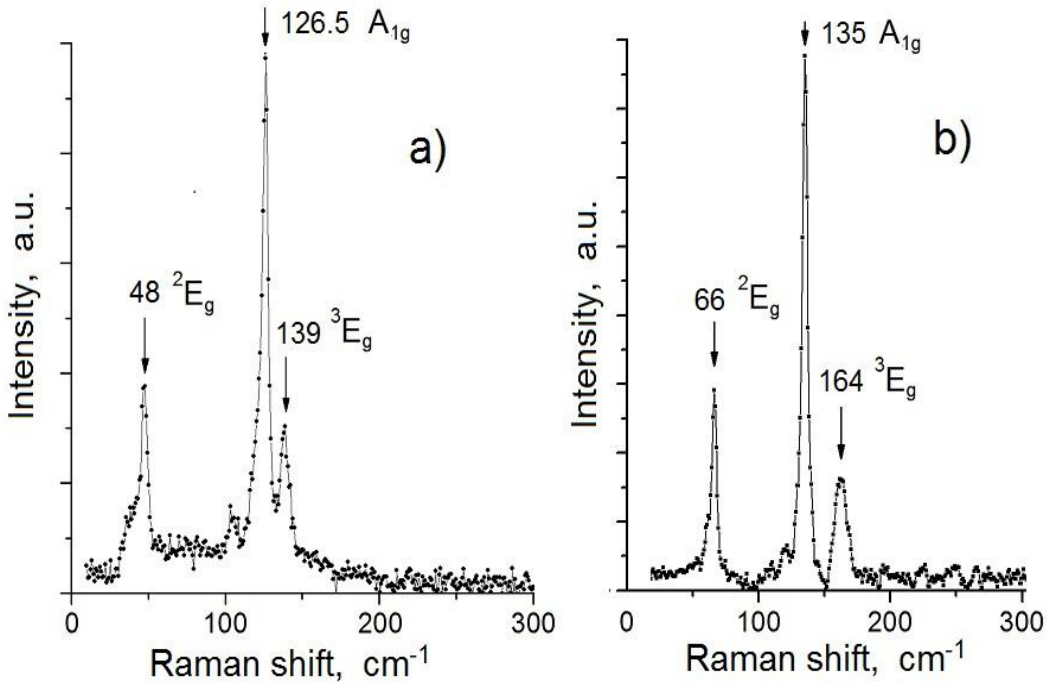

Fig. 2. Raman spectra of $TlInTe_2$ (a) and $TlGaTe_2$ (b) single crystals.

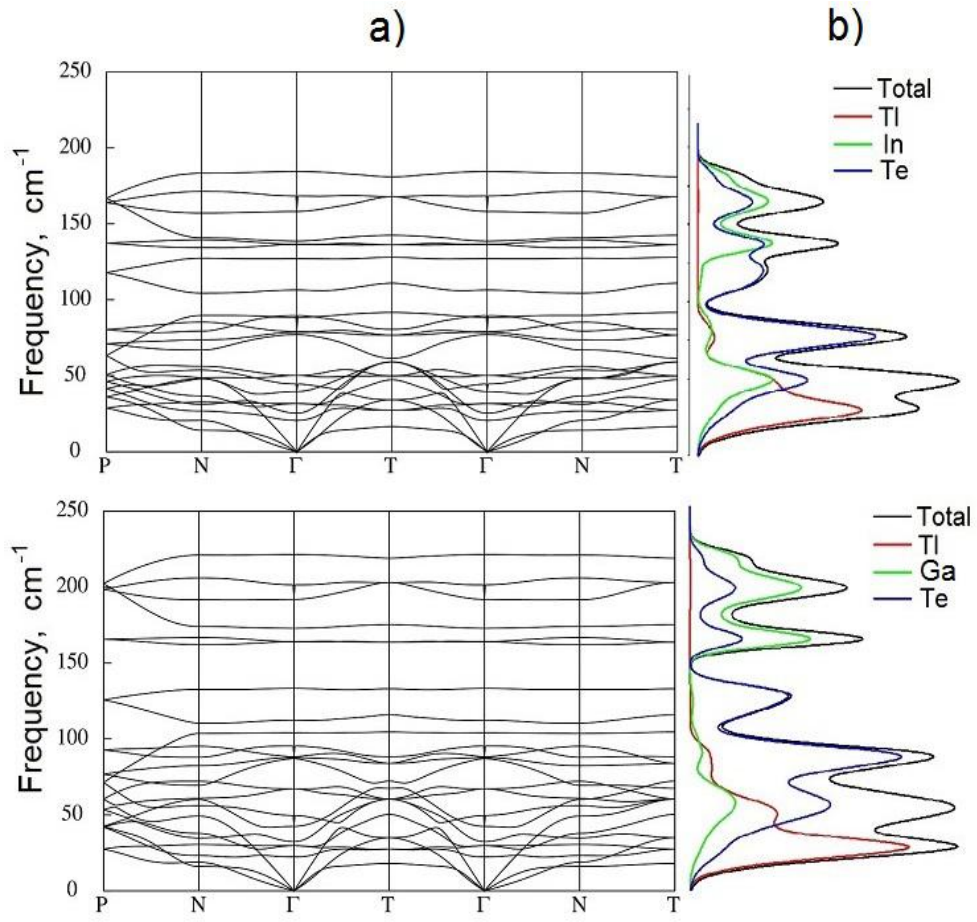

Fig. 3. Phonon spectra (a) and partial densities of states (b) of $TlInTe_2$ and $TlGaTe_2$ crystals.

Table 1.

Frequencies of experimentally recorded (ωexper) and theoretically calculated (ω_{cal}) R-active modes of $TlGaTe_2$, $TlInTe_2$ crystals in the center of the Brillouin zone and their symmetries

Modes	$TlGaTe_2$						$TlInTe_2$				
	ω calcul (cm^{-1})				ω exper (cm^{-1})		ω calcul (cm^{-1})		ω exper (cm^{-1})		
	[32]	[9]	[6]	This work	[31]	This work and [32]	[9]	This work	[31]	[6]	This work
^1E_g	16	38	19	31.6	-	-	30	33.4	-	-	-
^2E_g	60	58	60	69	67	66	42	51	48	49.3	48
B_{1g}	76	80	76	88	-	-	72	80	-	-	-
$^1B_{2g}$	99	99	99	104	-	-	83	88	-	-	-
A_{1g}	125	135	128	134	135	135	128	127	127	126.7	126.5
^3E_g	152	168	157	165	165	164	139	137	138	138	139
$^2B_{2g}$	210	230	216	222	-	-	189	184.5	-	-	-

Defects at the Tl sites would have little effect on these modes, although tellurium vibrations contribute to all three experimentally recorded modes. Defects associated with Te atoms will have the strongest effect on the A_{1g} mode at a frequency of 125-135 cm^{-1} (Fig. 3b). The above is confirmed by the results of our studies of the Raman spectrum of $TlInTe_2$ crystals doped with 5 at.% Fe [19], presented below. In the studied solid solutions, the local random distribution of In and Fe atoms associated with Te atoms will lead to fluctuations in the masses and force constants, and, as a result, to changes in the Raman spectrum and the appearance of a mode with a frequency of 120 cm^{-1} (Fig. 4b).

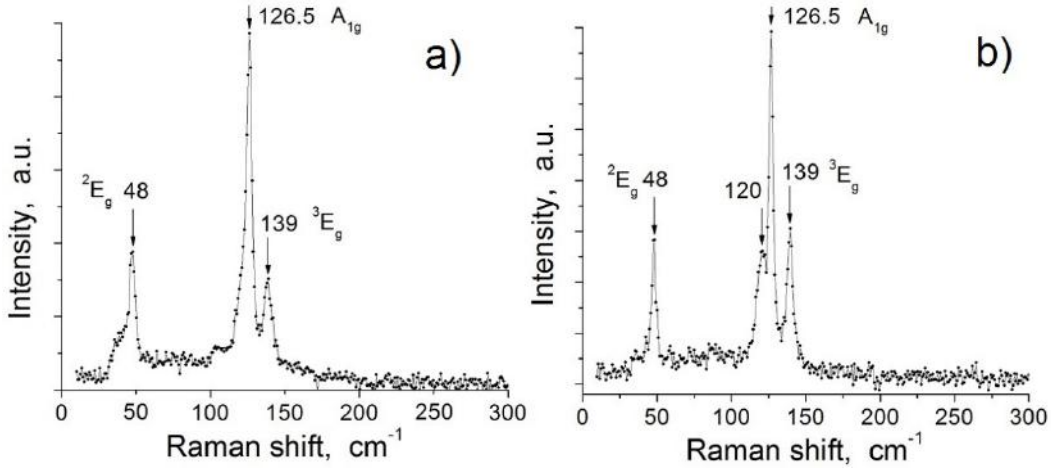

Fig. 4. Raman scattering spectra of single crystals: a) $TlInTe_2$; b) $TlInTe_2$ doped with 5.0 at.% Fe

3.2. Elastic constants of $TlInTe_2$ and $TlGaTe_2$ crystals

We calculated the elastic constants of $TlInTe_2$ and $TlGaTe_2$ crystals from first principles. It is well known that stresses and strains are described by second-rank tensors (σ_{ij} and ε_{kl}) in three-dimensional space and have nine components each. Within the framework of the generalized Hooke's law (2), they are related by a fourth-rank tensor C_{ijkl}, called the elasticity tensor, which generally contains 81 coefficients (elastic constants):

$$\sigma_{ij}=C_{ijkl}\varepsilon_{kl} \quad (2)$$

The requirement for the stress and strain tensors (2) to be symmetric reduces the number of independent elastic constants to 36.

$$C_{ijkl}=C_{jikl}=C_{ijlk}=C_{jilk} \quad (3)$$

Considering that the elastic strain energy W:

$$W=\frac{1}{2}C_{ijkl}\varepsilon_{ij}\varepsilon_{kl} \quad (4)$$

From this it follows that $C_{ijkl}=C_{klij}$ and the number of independent elastic constants decreases to 21. Thus, in the most general case of low-symmetry crystals, there

are 21 independent components of the elasticity tensor.

Furthermore, taking into account the symmetry of a specific crystal lattice allows for an even more significant reduction in the number of independent elastic constants. For example, more highly symmetric crystals with tetragonal symmetry are described by six elastic constants C_{11}, C_{12}, C_{13}, C_{33}, C_{44}, C_{66} [34-36].

According to the notation of W. Voigt, the elements of the elasticity tensor C_{ijkl} can be written using the following substitution of indices 11→1, 22→2, 33→3, 23,32→4, 12,21→6, in the form of a 6×6 matrix:

$$\begin{bmatrix} C_{11} & C_{12} & C_{13} & \ldots & 0 & \ldots & 0 & \ldots & 0 \\ C_{12} & C_{11} & C_{13} & \ldots & 0 & \ldots & 0 & \ldots & 0 \\ C_{13} & C_{13} & C_{33} & \ldots & 0 & \ldots & 0 & \ldots & 0 \\ 0 & \ldots & 0 & \ldots & C_{44} & \ldots & 0 & \ldots & 0 \\ 0 & \ldots & 0 & \ldots & 0 & \ldots & C_{44} & \ldots & 0 \\ 0 & \ldots & 0 & \ldots & 0 & \ldots & 0 & \ldots & C_{66} \end{bmatrix} \quad (5)$$

In crystals, certain relationships must be satisfied between the elastic constants, which follow from the equilibrium condition of the crystal lattice, the main requirement of which is the minimum energy density. These relationships, called the Born-Huang stability criteria, stem from the need to satisfy the stability criterion of the crystal lattice [37]. For the lattice to be stable, the energy density must be a positive-definite quadratic form such that the energy increases with any small deformation. If we arrange the coefficients of the quadratic form in the form of matrix (5) without the elastic constant C_{16}, then, according to a well-known theorem of algebra, this quadratic form is positive-definite if the determinants of all matrices of successive ranks (principal minors) are positive. That is, must be positive C_{66}, $C_{44}C_{66}$, $C_{44}^2C_{66}$, $C_{33}C_{44}^2C_{66}$, $(C_{11}C_{33}-C_{13}^2)C_{44}^2C_{66}$, $(C_{11}-C_{12})(C_{11}C_{33}+C_{12}C_{33}-2C_{13}^2)$. Thus, the following conditions must be met:

$$C_{11}>0;\quad C_{44}>0;\quad C_{66}>0;\quad C_{11}-C_{12}>0$$

$$C_{11}C_{33}-C_{13}^2>0 \quad (6)$$

$$C_{11}C_{33}+C_{12}C_{33}-2C_{13}^2>0$$

Similar relationships for crystals with hexagonal symmetry are presented in [38].

Table 2 presents the elastic constants C_{11}, C_{12}, C_{13}, C_{33}, C_{44} and C_{66} of $TlInTe_2$ and $TlGaTe_2$ crystals, calculated from first principles, as well as published data on the elastic constants C_{ij} of $TlInTe_2$, $TlGaTe_2$, and $TlInSe_2$. As can be seen from Table 2, replacing the Se anion with Te decreases the elastic constants, while replacing the In cation with Ga strengthens the bonds in the crystals.

Table 2.

The values of elastic constants C_{ij} of tetragonal $TlInTe_2$ and $TlGaTe_2$ crystals in GPa (in square brackets is a link to the work from which the data was taken).

Crystals	Reference	Elastic constants, in GPa					
		C_{11}	C_{12}	C_{13}	C_{33}	C_{44}	C_{66}
$TlGaTe_2$	This work	46.99	22.34	21.08	80.32	19.57	14.99
$TlInTe_2$	This work	48.2	21.24	20.46	71.79	19.12	16.69
$TlInSe_2$	[39]	42.11	12.59	8.93	83.54	11.88	11.24
$TlInSe_2$	[4]	59,82	22,07	30,03	84,56	15,92	13,87
$TlGaTe_2$	[6]	32,21	15,89	11,96	58,19	10,24	12,01
$TlGaTe_2$	[9]	40.9	19.8	17.1	68.1	13.3	16.1
$TlInTe_2$	[9]	39.6	18.1	16.4	60.8	14.5	15.3
$TlInTe_2$	[7]	20.9	15.66	12.64	58.3	16.2	16.44

3.3. Elastic moduli of $TlInTe_2$ and $TlGaTe_2$ crystals

In practice, along with elastic constants, bulk elastic moduli B are widely used, for example, when calculating Grüneisen parameters [40], coefficients of volumetric thermal expansion, thermodynamic quantities, and other anharmonic effects [41, 42]. By definition, bulk elastic moduli are determined from the relationship:

$$W = \frac{1}{2} B \xi^2 \quad (7)$$

Here the volumetric strain is related to the diagonal components of the strain tensor ε_{ii} by the relation

$$\frac{\xi}{3} = \varepsilon_{11} + \varepsilon_{22} + \varepsilon_{33} \quad (8)$$

From (4) and (7), taking into account (8), it is easy to obtain the relationship between the bulk modulus of elasticity and the elastic constants for crystals of tetragonal symmetry:

$$B_V = \frac{1}{9}(2C_{11} + C_{33} + 2C_{12} + 4C_{13}) \quad (9)$$

An expression similar to (9) for the bulk modulus of elasticity B in the Voigt bound approximation of crystals with tetragonal symmetry is given in [43, 44]. In the case of crystals with cubic symmetry with $C_{11}=C_{33}$ and $C_{12}=C_{13}$, expression (9) transforms into a relationship between the bulk

modulus of elasticity and the elastic constants for crystals with cubic symmetry:

$$B = \frac{1}{3}(C_{11} + 2C_{12}) \quad (10)$$

According to the data [43, 44], the Voigt shear modulus G_V is equal to

$$G_V = \frac{1}{30}(M + 3C_{11} - 3C_{12} + 12C_{44} + 6C_{66}) \quad (11)$$

where, $M=C_{11}+C_{12}+2C_{33}-4C_{13}$

The value of the bulk modulus of elasticity B_R in the Reuss approximation (Reuss bound) of crystals with tetragonal symmetry [43, 44]:

$$B_R=C^2/M \ , \qquad C^2= (C_{11}+C_{12}) \cdot C_{33}-2C_{13}^2 \quad (12)$$

The value of the shear modulus G_R in the Reuss approximation (Reuss bound) of crystals with tetragonal symmetry [54, 55]:

$$G_K = 15\left\{\frac{18B_V}{C^2} + \left[\frac{6}{(C_{11} - C_{12})}\right] + \frac{6}{C_{44}} + \frac{3}{C_{66}}\right\}^{-1} \quad (13)$$

Using energy considerations, Hill proved [45], that the Voigt and Reuss equations represent upper and lower limits on the true polycrystalline constants, and he recommended that the practical estimate of polycrystalline moduli be the arithmetic mean of the extreme values. The Voigt bound is obtained from the average polycrystalline moduli based on the assumption of uniform strain throughout the polycrystal and is the upper limit of the actual effective moduli, while the Reuss bound is obtained by assuming uniform stress and is the lower limit of the actual effective moduli. The arithmetic mean of the Voigt and Reuss bounds is called the Voigt-Reuss-Hill approximation [45]. In terms of the Voigt-Reuss-Hill approximations

$$B=(B_V+B_R)/2 \ , \ G=(G_V+G_R)/2 \quad (14)$$

Young's modulus (Young's modulus E) is defined as

$$E = 9BG/(3B + G) \quad (15)$$

And the Poisson's ratio is calculated using the following formula:

$$\nu = (3B - 2G)/[2(3B + G)] \quad (16)$$

The values of elastic moduli and Poisson's ratios of $TlInTe_2$ and $TlGaTe_2$ crystals calculated by us from relations (9) - (16), as well as known data from the literature [4, 6, 7, 9], are presented in Table 3.

Table 3.

The values of elastic modulus and Poisson's ratio $TlInTe_2$ and $TlGaTe_2$ crystals

Compounds	Elastic modulus, GPa							Poisson's ratio, ν
	Bulk Voigt, B_V	Bulk Reuss, B_R	Bulk, B	Shear Voigt, G_V	Shear Reuss, G_R	Shear, G	Young's, E	
$TlGaTe_2$ This work	33.7	32.13	33	18.15	16.03	17.1	43.8	0.28
$TlInTe_2$ This work	32.5	31.6	32	18.05	17.5	17.8	45	0.27
$TlInSe_2$ [4]	-	-	40	-	-	17	44.7	0.31
$TlGaTe_2$ [6]	-	-	22	-	-	20	46	0.15
$TlGaTe_2$ [9]	-	-	28.1	-	-	15	38.3	0.27
$TlInTe_2$ [9]	-	-	26.5	-	-	14.7	37.2	0.27
$TlInTe_2$ [7]	-	-	19	-	-	10.8	27.2	0.26

4. CONCLUSION

This paper presents the results of a study of the phonon properties of $TlInTe_2$ and $TlGaTe_2$ crystals. The phonon properties of $TlInTe_2$ and $TlGaTe_2$ crystals were investigated experimentally using Raman scattering. The Raman spectra of $TlInTe_2$ crystals revealed spectral lines at 48 cm^{-1} (^2E_g), 126.5

cm^{-1} (A_{1g}) and 139 cm^{-1} (^3E_g), while those of $TlGaTe_2$ crystals revealed lines at 66 cm^{-1} (^2E_g), 135 cm^{-1} (A^1_g), and 164 cm^{-1} (^3E_g).

The experimentally obtained frequencies are in good agreement with theoretically calculated ones. Optical mode dispersion was calculated from first principles, and the partial densities of states (PDOS) projected onto atoms and optical phonon frequencies were determined. It was found that the dispersion of optical phonons in all symmetric directions except the PN line is insignificant, indicating weak interatomic interactions in these directions. Furthermore, the presence of lighter Ga atoms shifts the phonon spectra of the $TlGaTe_2$ compound toward higher frequencies (>200 cm^{-1}). The presented partial phonon densities of states for $TlInTe_2$ and $TlGaTe_2$ crystals show that the main contribution at low frequencies comes from the heaviest atoms, at medium frequencies from Te atoms, and at high frequencies from In and Ga atoms. Analysis of the calculated results indicates that substituting gallium atoms for indium atoms in the compounds should experimentally manifest itself in behavior with changes in the composition of the ^2E_g and ^3E_g modes.

It is shown that defects associated with Te atoms will have the strongest effect on the A^1_g mode at a frequency of 125-135 cm^{-1}. The above is confirmed by the results of our studies of the Raman spectrum of $TlInTe_2$ crystals doped with 5 at.% Fe [19]. In the studied solid solutions, the local random distribution of In and Fe atoms bound to Te atoms will lead to fluctuations in the masses and force constants, and, as a result, to changes in the Raman spectrum and the appearance of a mode with a frequency of 120 cm^{-1}.

The values of six elastic constants C_{11}, C_{12}, C_{13}, C_{33}, C_{44} and C_{66} of the $TlInTe_2$ and $TlGaTe_2$ compounds were also calculated from first principles. The relationships between the elastic constants corresponding to the condition of crystal lattice stability for crystals with tetragonal symmetry are presented. The bulk modulus, shear and Young's moduli, and Poisson's ratio were determined in the Voigt-Reuss-Hill approximation.

CONFLICT OF INTEREST

The authors declare that they have no conflict of interest.

[1] *H. Hahn, B. Wellmann*, "Über ternäre Chalkogenide des Thalliums mit Gallium und Indium," Naturwissenschaften, 1967, vol. 54, p. 42.

[2] *D. Müller, G. Eulenberger, and H. Hahn*, "Über ternare Thallium chalkogenide mit thalliums selennid structur," Zeitschriftfür anorganische und allgemeine Chemie, 1973, vol. 398, № 2, pp. 207-220.

[3] *S. Yesudhas, N. Yedukondalu, M. K. Jana, J. Zhang, J. Huang, B. Chen, H. Deng, R. Sereika, H. Xiao, S. Sinogeikin, C. Kenney-Benson, K. Biswas, J. B. Parise, Y. Ding, and H. Mao*, "Structural, Vibrational, and Electronic Properties of 1D-$TlInTe_2$ under High Pressure: A Combined Experimental and Theoretical Study," Inorganic Chemistry, 2021, vol. 60, № 13, pp. 9320-9331.

[4] *S.H. Jabarov, N.A. Ismayilova, D.P. Kozlenko, T.G.Mammadov, N.T.Mamedov, H.S.Orudzhev, S.E. Kichanov, F.A. Mikailzade, E.K. Kasumova, N.T. Dang*, "Structural and elastic properties of $TlInSe_2$ at high pressure," Solid State Sciences, 2021, vol. 111, 106343.

[5] *N.T. Mamedov, S.H. Jabarov, D.P. Kozlenko, N. A. Ismayilova, M.Yu. Seyidov, T.G. Mammadov, and N.T. Dang*, "Neutron diffraction study of the crystal structure of $TlInSe_2$ at high pressure," International Journal of Modern Physics B, 2019, vol. 33, № 15, 1950149.

[6] *M. Rasukkannu, D. Velauthapillai, P. Vajeeston*, "First-Principle Calculation of High Absorption - $TlGaTe_2$ for Photovoltaic Application," Materials, 2019, vol. 12**,** № 17, 2667.

[7] *T. Helaimia, S. Maabed, A. Benmakhlouf, A. Bouhemadou, F. Fares, M. Bouchenafa, A. Bentabet and S. Bin-Omran*, "Comprehensive DFT investigation of ternary Thallium tetragonal Crystals: Assessing their viability for solar cell applications," Physica Scripta, 2024, vol. 99, № 4, 045931.

[8] *Y.G. Shim, T. Asahi, K. Wakita, N.T. Mamedov, E.N. Aliyeva, and N.A. Abdullayev*, "Photoinduced Reversible Local Deformation of the Surface Relief in Bulk Single Crystals of $TlInSe_2$, $TlGaTe_2$, and TlSe," Technical Physics Letters,2018,vol. 44, № 7, pp.643–645.

[9] *M. Wu, Enamullah, and Li Huang*, "Unusual lattice thermal conductivity in the simple crystalline compounds $Tl\mathit{X}Te_2$ (X = Ga, In)," Phys. Rev. B, 2019, vol. 100, 075207.

[10] *M.K. Jana, K. Pal, A. Warankar, P. Mandal, U.V. Waghmare, and K. Biswas*, "Intrinsic rattler-induced low thermal conductivity in Zintl type $TlInTe_2$," J. Amer. Chem. Soc., 2017, vol. 139, № 12, pp. 4350-4353.

[11] *H. Matsumoto, K. Kurosaki, H. Muta, and S. Yamanaka*, "Systematic investigation of the thermoelectric properties of $Tl\mathit{M}Te_2$ (M = Ga, In, or Tl)," J. Appl. Phys., 2008, vol. 104, № 7, 073705.

[12] *M. Dutta, M. Samanta, T. Ghosh, D.J. Voneshen, K. Biswas*, "Evidence of Highly Anharmonic Soft Lattice Vibrations in a Zintl Rattler," Angewandte Chemie, 2021, vol. 60, № 8, pp. 4259-4265.

[13] *F.N. Abdullayev, T.G. Kerimova, and N.A. Abdullayev*, "Conductivity Anisotropy and Localization of Charge Carriers in $TlInTe_2$ Single Crystals," Phys. Solid State, 2005, vol. 47, № 7, pp. 1221–1224.

[14] *N. Mamedov, K. Wakita, A. Ashida, T. Matsui, and K. Morii*, "Super thermoelectric power of one-dimensional $TlInSe_2$," Thin Solid Films, 2006, vol. 499, № 1-2, pp. 275-278.

[15] *R.R. Guseynov, V.A. Tanriverdiyev, G. Kipshidze, Y.N. Aliyeva, Kh.V. Aliguliyeva, N.A. Abdullayev, and N.T. Mamedov*, "$InAs_{1-x}Sb_x$ Heteroepitaxial Structures on Compositionally Graded GaInSb and AlGaInSb Buffer Layers, Semiconductors," 2017, vol. 51, № 4, pp. 524–530.

[16] *I.R. Amiraslanov, Z.S. Aliev, P.A. Askerova, E.H. Alizade, Y.N. Aliyeva, N.A. Abdullayev, Z.A. Jahangirli, M.M. Otrokov, N.T. Mamedov, and E.V. Chulkov*. "Crystal structure and Raman-active lattice vibrations of magnetic topological insulators $MnBi_2Te_4 \cdot n(Bi_2Te_3)$ (n = 0, 1,...,6)," Phys. Rev. B, 2022, vol. 106, № 18, 184108.

[17] *A.I. Najafov, G.R. Mahmudova, Z.A. Jahangirli, V.B. Aliyeva, Z.I. Badalova, T.G. Mammadov, and N.A. Abdullayev*, "Raman Scattering in $TlGa_xIn_{1-x}Te_2$ Solid Solutions: Experiment and Calculations from First Principles," Phys. Wave Phen., 2025, vol. 33, № 2, pp. 117–126.

[18] *N.A. Abdullayev, I.R. Amiraslanov, Z.S. Aliev, Z.A. Jahangirli, I.Yu. Sklyadneva, E.G. Alizade, Y.N. Aliyeva, M.M. Otrokov, V.N. Zverev, N.T. Mamedov, and E. V. Chulkov*, "Lattice Dynamics of Bi_2Te_3 and Vibrational Modes in Raman Scattering of Topological Insulators $MnBi_2Te_4 \cdot n(Bi_2Te_3)$," JETP Letters, 2022, vol. 115, № 12, pp. 749-756.

[19] *A.I. Najafov, N.N. Mursakulov, M.M. Shirinov, T.G. Mammadov, I.A. Mamedova, and N.A. Abdullayev*, "Study of the Physicochemical Properties of the $TlInTe_2$–Fe System," Phys. Solid State, 2025, vol. 67, № 8, pp. 635–641.

[20] *Z.A. Jahangirli, I.Q. Qasimoglu, Kh.A. Hidiyev, I.A. Mamedova, J.A. Guliyev, S.S. Ragimov, T.G. Mammadov, and N.A. Abdullayev*, "Ab Initio Calculations and Experimental Spectral Ellipsometry Study of the Electronic Properties of $CuInS_2$ Crystals," Phys. Wave Phenomena, 2025, vol. 33, № 1, pp. 36–45.

[21] *Z.S. Aliev, E.H. Alizade, D.A. Mammadov, J.N. Jalilli, Y.N. Aliyeva, N.A. Abdullayev, S.S. Ragimov, S.M. Bagirova, S. Jahangirov, N.T. Mamedov, E.V. Chulkov*, "Spectroscopic ellipsometry and raman spectroscopy of $Bi_{1-x}Sb_xTeI$ solid solutions with $x \leq 0.1$," Thin Solid Films, 2023, vol. 768, 139727.

[22] *N.T. Mamedov, E.H. Alizade, Z.A. Jahangirli, Z.S. Aliyev, N.A. Abdullayev, S. N. Mammadov, I.R. Amiraslanov, Y. Shim, K. Wakita, S.S. Ragimov, A.I. Bayramov, M.B. Babanly, A.M. Shikin, E. V. Chulkov*, "Infrared spectroscopic ellipsometry and optical spectroscopy of plasmons in classic 3D topological insulators," J. Vac. Sci. Technol. B, 2019, vol. 37, № 6, 062602.

[23] *I.Q. Qasimoglu, Z.A. Jahangirli, I.A. Mamedova, G.S. Mehdiyev, Z.I. Badalova, R.A. Hasanova, S.S. Osmanova, Kh.V. Aliguliyeva, B.H. Mehdiyev, and N.A. Abdullayev*, "Phonon Properties of $CuInS_2$ Crystals: Experiment and First-Principles Calculations," Phys. Solid State, 2025, vol. 67, № 11, pp. 968–976.

[24] *P. Gianozzi, S. de Gironcoli, P. Pavone, S. Baroni*, "Ab initio calculation of phonon dispersions in semiconductors," Phys. Rev. B, 1991, vol. 43, № 9, pp. 7231-7242.

[25] *S. Baroni, S. de Gironcoli, A. Dal Corso, P. Gianozzi*, "Phonons and related crystal properties from density-functional perturbation theory," Rev. Mod. Phys., 2001, vol. 73, № 2, pp. 515-562.

[26] *X. Gonze*, "First-principles responses of solids to atomic displacements and homogeneous electric fields: Implementation of a conjugate-gradient algorithm," Phys. Rev. B, 1997, vol. 55, № 16, pp. 10337-10354.

[27] *X. Gonze, J.M. Beuken, R. Caracas, F. Detraux, M. Fuchs. G. M. Rignanese, L. Sindic, M. Verstraete, G. Zerah, F. Jallet*, "First-Principles Computation of Material Properties: The ABINIT Software Project," Comput. Mater. Sci., 2002, vol. 25, pp. 478-492.

[28] *C. Hartwigsen, S. Goedecker, J. Hutter*, "Relativistic separable dual-space Gaussian pseudopotentials from H to Rn," Phys.Rev. B, 1998, vol. 58, № 7, pp. 3641-3662.

[29] *J.P. Perdew and A. Zunger*, "Self-interaction correction to density-functional approximations for many-electron systems," Phys. Rev. B, 1981, vol. 23, № 10, pp. 5048–5079.

[30] *H. J. Monkhorst, J. D. Pack*, "Special points for Brillonin-zone integrations," Phys. Rev. B**,** 1976, vol. 13, № 12, pp. 5188-5192.

[31] *N.M. Gasanly, A.F. Goncharov, B.M. Dzhavadov, N.N. Melnik, V.I. Tagirov, E.A. Vinogradov*, "Vibrational Spectra of $TlGaTe_2$, $TlInTe_2$, and $TlInSe_2$ Layer Single Crystals," Phys. Status Solidi B, 1980, vol. 97, № 1, pp. 367-377.

[32] *V. Jafarova, G. Orudzhev, R. Paucar, O. Alekperov, Y.G. Shim, K. Wakita, N.T. Mamedov, N.A. Abdullayev, and A. Najafov*, "Ab initio calculations of phonon dispersion and lattice dynamics in $TlGaTe_2$," Phys. Status Solidi C, 2015, vol. 12, № 6, pp. 664–667.

[33] *S. Ves*, **"**High-pressure Raman Study of the Chalcogenide $TlInTe_2$," Phys. Status Solidi B, 1990, vol. 159, № 2, pp. 699-706.

[34] *O. Gomis, R. Vilaplana, F. J. Manjon, D. Santamarıa-Perez, D. Errandonea, E. Perez-Gonzalez, J. Lopez-Solano, P. Rodrıguez-Hernandez, A. Munoz, I. M. Tiginyanu and V. V. Ursaki*, "High-pressure study of the structural and elastic properties of defect-chalcopyrite $HgGa_2Se_4$," Journal of Applied Physics, 2013, vol. 113, № 7, 073510.

[35] *I.A. Mamedova, Z.A. Jahangirli, T.G. Kerimova, and N.A. Abdullayev*, "Bulk

Modulus, Elastic Constants, and Force Constants of Interatomic Bonds of $II–III_2–VI_4$ Compounds", Phys. Status Solidi B, 2023, vol. 260, № 6, 2200441.

[36] *I.A. Mamedova, Z.A. Jakhangirli, S.S. Osmanova, and N.A. Abdullayev*, "Elastic Properties and Regularities in Frequencies of Optical Phonons of $A^{II}B^{III}{}_2C^{VI}{}_4$ Compounds," Phys. Solid State, 2024, vol. 66, № 11, pp. 529–536.

[37] *M. Born, K. Huang*, Dynamical Theory of Crystal Lattices, (Clarendon Press, Oxford, 1956).

[38] *N.A. Abdullayev*, "Elastic Properties of Layered Crystals," Phys. Solid State, 2006, vol. 48, № 4, pp. 663–669.

[39] *I. Martynyuk-Lototska, O. Mys, A. Say, I. Trach, D. Adamenko, O.O. Gomonnai, I. Roman, R. Vlokh*, Phase Transitions, "Anisotropy of acoustic and thermal expansion properties of $TlInSe_2$ crystals", 2019, vol. 92, № 1, pp. 23-35.

[40] *N.A. Abdullayev*, "Grüneisen Parameters for Layered Crystals," Phys. Solid State, 2001, vol. 43, № 4, pp. 727–731.

[41] *Z.I. Badalova, N.A. Abdullayev, G.H. Azhdarov, Kh.V. Aliguliyeva, S.Sh. Gahramanov, S.A. Nemov and N.T. Mamedov*, "Anharmonicity of Lattice Vibrations in Bi_2Se_3 Single Crystals," Semiconductors, 2019, vol. 53, № 3, pp.291–295.

[42] *Kerimova T.G., Mamedov Sh.S., Mamedova I.A.*, "Deformation potentials of the Γ (000) band extrema in $CdGa_2S_4$," Semiconductors, 1998, vol. 32, № 2, pp. 133–135.

[43] *Z. Wu, E. Zhao, H. Xiang, X. Hao, X. Liu, and J. Meng*, "Crystal structures and elastic properties of superhard IrN_2 and IrN_3 from first principles," Phys. Rev. B, 2007, vol. 76, 059904.

[44] *J.P. Watt, L. Peselnick*, "Clarification of the Hashin-Shtrikman bounds on the effective elastic moduli of polycrystals with hexagonal, trigonal, and tetragonal symmetries," J. Appl. Phys., 1980, vol. 51, № 3, pp. 1525–1531.

[45] *R. Hill*, "The Elastic Behaviour of a Crystalline Aggregate," Proceedings of the Physical Society. Section A, 1952, vol. 65, № 5, pp. 349-354.

Received: 03.11.2025